Restructuring of Hydration Shells Rules the Low-Temperature Dynamics of B-DNA via Its Two Conformer Substates

Arthur Pichler, Simon Rüdisser, Christine Rauch, Wolfgang Flader, Bernd Wellenzohn, Rudolf H. Winger, Klaus R. Liedl, Andreas Hallbrucker, and Erwin Mayer*

Institut für Allgemeine, Anorganische und Theoretische Chemie, Universität Innsbruck, A-6020 Innsbruck, Austria

Received: August 10, 2001; In Final Form: December 20, 2001

The low-temperature dynamics in nonoriented hydrated films of the sodium salt of the d(CGCGAATTCGCG)$_2$ dodecamer with either 13 (14) or 8 water molecules per nucleotide ($\Gamma = 13$ (14) or 8) was studied by Fourier transform infrared (FTIR) spectroscopy. This dodecamer is ideal for this study because it remains in the B form even at low water activity, and thus, we do not have to worry about IR bands from the A form. The effects of cooling rate and of isothermal relaxation at 180 and 200 K on B-DNA's conformer substates, B_I and B_{II}, were revealed by a combination of IR difference spectroscopy and by determining B_{II}/B_I population ratios via careful curve resolution of IR spectra. On slow cooling a dodecamer film with $\Gamma = 13$ (14) from 290 to 180 K at a rate of 2 K min^{-1}, B_{II} transforms into B_I fast enough to remain equilibrated down to 180 K. However, on fast-cooling of the same sample at a rate of ≈60 (or 90) K min^{-1}, a nonequilibrium state is frozen-in. Unexpectedly, on isothermal relaxation at 180 or 200 K toward equilibrium, B_I converts into B_{II}; that is, the B_{II}/B_I equilibrium line is approached from below. This isothermal $B_I \rightarrow B_{II}$ transition is coupled with restructuring of their hydration shells such that increased hydrogen-bond interaction stabilizes B_{II}. A dodecamer film with $\Gamma = 8$ behaves very differently: the B_{II}/B_I population ratio remains equilibrated both on slow-cooling and on fast-cooling to 180 K, and thus, isothermal relaxation does not occur. Therefore, the falling-out of equilibrium on fast-cooling of the dodecamer with $\Gamma = 13$ (14) must be caused by one or more of these additional water molecules. We conclude that, with these additional water molecules as part of the hydration shells, restructuring of the B_I and B_{II} hydration shells is a comparably slow process, whereas $B_{II} \rightarrow B_I$ is much faster. In this scenario, first restructuring of the hydration shells slows down on fast-cooling, and the B_{II}/B_I equilibrium line is left at ≈240−220 K. However, the $B_{II} \rightarrow B_I$ transition continues until a B_{II}/B_I ratio is frozen-in which is below that of the B_{II}/B_I equilibrium ratio. Because the frozen-in hydration shells cannot stabilize B_{II} anymore by additional hydrogen bonding, the B_I state is favored in the frozen-in nonequilibrated state. We further show that the less complete IR-spectroscopic analysis of a native polymeric DNA with $\Gamma = 13$ reveals the same effects as the dodecamer and, thus, that our conclusions seem to be general and not restricted to the synthetic oligonucleotide. Isobestic points in the IR spectra of the dodecamer and of native polymeric B-DNA recorded on isothermal relaxation at 200 K indicate that only two species are involved. Thus, the low-temperature dynamics of B-DNA seems to be caused solely by the processes described above. Our findings enable us to interpret the inelastic neutron scattering spectroscopy analysis reported by Sokolov et al. (*J. Chem. Phys.* **1999**, *110*, 7053−7057), and they support their speculation that the glassy dynamics in DNA is ruled by water of hydration. We further speculate that slowing down of restructuring of the B_I and B_{II} hydration shells at ≈220−240 K is the cause for the suppression of the biological functions at low temperatures.

Introduction

It is well-known that water is not just a medium to keep DNA dissolved; it interacts with the solute, and the distribution of water molecules in the first hydration shell is sensitive to the A- or B-type conformation of DNA (for reviews see refs 1−6). Berman and Schneider[6] emphasized in their recent review of nucleic acid hydration that "there is an accumulating body of evidence suggesting that water plays a key role in modulating the conformations, interactions, and recognition properties of nucleic acids". Pronounced changes in hydration also occur on interconversion between the conformer substates (CSs) of B-DNA, B_I and B_{II}. In our studies of hydrated films and aqueous solutions of the Drew−Dickerson dodecamer (DDD), d(CGCGAATTCGCG)$_2$, by Fourier transform infrared (FTIR) spectroscopy[7−13] and computer simulation,[14−16] we observed that the B_{II} conformer substate is much more populated in nonoriented films than in the single crystal and that the B_{II} substate population increases with decreasing water activity.[11,16] Pronounced IR spectral changes upon $B_I \rightarrow B_{II}$ interconversion are consistent with migration of water from ionic phosphate toward the phosphodiester and/or sugar moieties.[7−13] This agrees with our recent molecular dynamics (MD) simulation of the B_I and B_{II} substates in DDD, where analysis of radial distribution functions revealed that water migrates on $B_I \rightarrow B_{II}$ transition from ionic phosphate toward the sugar ring oxygen.[14−16] Thus, water exchange is coupled to the conformational $B_I \rightarrow B_{II}$ transition, and differences in hydration in the form of enhanced hydrogen-bond interaction seem to be the driving force for the $B_I \rightarrow B_{II}$ transition. We observed similar behavior in our FTIR

* To whom correspondence should be addressed.

10.1021/jp013121+ CCC: $22.00
Published on Web 03/05/2002

spectroscopic study of highly polymeric native B-DNA from salmon testes, in that in addition to the canonical (B_I) form of B-DNA, unexpectedly high population of B_{II} occurs and water migration is observed on $B_I \rightarrow B_{II}$ transition in the same manner as for DDD.[7−10,12]

Here we show that B-DNA's low-temperature dynamics is ruled by restructuring of the hydration shells of the conformer substates. Incentive for this study was to understand our previous unexpected observation that B_{II} converts into B_I on slow cooling from 290 K, whereas B_I converts into B_{II} on isothermal relaxation of fast-cooled films at 200 K.[7−13] We had tentatively attributed this reversal of CSs interconversion to a minimum in the equilibrated B_{II}/B_I conformer population ratios at low temperatures, in the same manner reported for the CO conformer populations of carbonylmyoglobin[17] and carbonylhemoglobin.[18] However, this idea had to be abandoned in further studies, and we show here that restructuring of hydration shells of the B_I and B_{II} conformer substates of B-DNA is the cause for reversal of conformer interconversion. This restructuring is at low temperatures a comparatively slow process, and thus, it can rule the much faster interconversion of B-DNA's CSs. The key to this study is to decrease the hydration level in DDD films from 13 (14) to 8 water molecules per nucleotide ($\Gamma = 13$ (14) or 8) and to investigate the effects of cooling rate and of isothermal relaxation on B-DNA's conformer substates distribution in dependence of hydration level. The B_{II}/B_I population ratios were determined by a combination of IR difference spectroscopy and careful curve resolution of IR spectra.[13]

Our method for investigating the dynamics and interconversion of CSs in B-DNA by FTIR spectroscopy was described recently,[7−13] and it is outlined briefly as follows. At ambient temperature, the B_I and B_{II} conformer substates of B-DNA interconvert rapidly in aqueous solution or in nonoriented hydrated films.[19−22] On cooling into the glassy state, the rate of CSs interconversion first slows down and eventually approaches zero. Because the equilibrium constant for $B_I \leftrightarrow B_{II}$ interconversion varies with temperature, a nonequilibrium distribution of CSs is generated by rapid quenching into the glassy state. On heating to an appropriate temperature in the glass $\rightarrow$ liquid transition region, *isothermal* relaxation toward equilibrium can be followed either by differential scanning calorimetry (DSC)[9,12,23,24] or by FTIR spectroscopy.[7−13] This is the basis of our approach for investigating the onset of molecular motions by calorimetric enthalpy relaxation and its recovery and by distinguishing between the IR spectral features of interconverting conformers. We have further tested this approach with chlorocyclohexane where equilibration via axial $\rightarrow$ equatorial conformer interconversion could be observed isothermally in the glass $\rightarrow$ liquid transition region.[25] Recently, we have shown by FTIR spectroscopy that, in nonoriented hydrated films of DDD and of native B-DNA from salmon testes, the same B_I and B_{II} CSs are involved in relaxation toward equilibrium and that at 200 K B_I interconverts into B_{II}.[8−10,12] The spectral changes become observable in the form of IR difference spectra where positive peaks indicate the formation of B_{II} and negative peaks the disappearance of B_I. The advantage of following relaxation via conformer substate interconversion isothermally is that changes in band shape and position with temperature are avoided. When an experimentally convenient temperature is selected, where relaxation time is between minutes and hours, interconversion of conformers can be followed by conventional FTIR spectroscopy.[7−13]

The IR spectroscopic details of the estimation of B_I to B_{II} conformer substate population ratios via curve resolution of IR spectra recorded either isothermally at 200 K or at ambient temperatures are described in ref 13. DDD was selected for our studies because it is the best characterized oligonucleotide,[26−30] and it persists in the B-form even at low water activity.[31] Therefore, problems with formation of A-DNA with decreasing water activity are avoided. DDD was the first B-type oligonucleotide for which the single-crystal structure had been determined by X-ray diffraction.[26−30] It contains the recognition site of the *Eco*RI restriction enzyme, and because of its biological importance, it remained at the focus of biophysical studies up to now. It has been studied among others by NMR,[21,22,32−36] Raman,[37−39] and IR spectroscopy,[8−13,40,41] by molecular modeling studies,[22,42−44] and by molecular dynamics (MD) simulation.[14−16,32,45−47] The B_I and B_{II} CSs involve changes in the phosphate backbone conformation about the C3′−O3′−P segment of the backbone chain, with the phosphate group rotating toward the minor groove in the B_{II} conformation.[48−51] In the B_I substate, the corresponding ϵ and ζ angles derived from X-ray structures are between 120−210° (trans) and 235−295° (gauche$^-$), and for B_{II}, the ϵ angle lies between 210 and 300° (gauche$^-$) and for ζ between 150 and 210° (trans). These CSs are frozen-in in the crystal but interconvert in solution at ambient temperature on a (sub)nanosecond time scale.[19−22] In the single crystal of DDD, B_{II} occurs at the G10 and G22 positions.[48,50,51] Therefore, the B_I to B_{II} population ratio is 10:1. Until recently, the B_{II} substate was considered to be the minority species and was even attributed to crystal packing effects.[52] However, our studies of nonoriented hydrated films of DDD have shown that the B_{II} population is higher than in the single crystal[8,10,13] and that it increases further with decreasing water activity.[11,16]

The growing importance of the B_{II} substate is demonstrated by two recent studies: first, Clark et al.[53] reported in a single crystal study of dehydrated DDD by X-ray diffraction that "the fully dehydrated structure contains an unusually high number of B_{II} backbone conformations", and second, van Dam and Levitt[54] showed by a combination of solid-state ^{31}P and ^{13}C NMR, X-ray diffraction, and model building that the C-form of DNA is simply a B_{II}-rich form of B-form DNA and, thus, "that the B to C transition in fibers corresponds to B_I to B_{II} conformational changes of the individual nucleotides". CSs of biologically active B-DNA could play a decisive role in nonspecific interaction of proteins with the DNA backbone: in this highly dynamic system, which fluctuates between B_I and B_{II} substates, a protein approaching B-DNA could select the B_I or B_{II} substate, depending on which one gives optimal interaction with the bases and the sugar−phosphate backbone.[8,21,48] The possible biological implications of enhanced B_{II} population for interaction with a protein has been discussed in recent papers.[8,21,22,54]

Our findings enable us to interpret the inelastic neutron scattering spectroscopy analysis reported by Sokolov et al.,[55] and they support their speculation that the glassy dynamics in DNA is ruled by water of hydration. We further surmize that the slowing down of the restructuring of the B_I and B_{II} hydration shells on cooling to $\approx$240−220 K is the cause for the suppression of B-DNA's biological functions at low temperatures.

We note that this study now enables us to interpret our DSC studies of native polymeric B-DNA, namely, the unexpected width of the glass transition region, the effect of hydration level and cooling rate, of annealing temperature and time on the shapes of the DSC plots, in terms of conformer substates

interconversion and restructuring of their hydration shells.[9,12,23,24] This will be reported separately.

Experimental Section

Materials. Lyophilized DDD was obtained as sodium salt from MWG BIOTECH and purified by HPLC or HPSF (high-purity salt-free).[8] The triethylammonium acetate buffer was removed by precipitation of DDD with cold ethanol. Quantitative removal of the buffer was controlled by the absence of the intense IR buffer bands at 1558 and 1414 cm^{-1}. HPSF purified DDD did not contain buffer. The sodium salt of DNA from salmon testes, NaDNA, was obtained from Fluka Chemical Company (No. 31163). As-received NaDNA contained according to its specification 12.9 wt % water and 0.08 wt % protein. It was characterized by its IR spectra for relative amounts of A- and B-DNA and by comparison with IR spectra reported by Taillandier et al.[56] The base pair length of NaDNA (No. 31163) was determined according to the method of Huber et al.[57] The broad distribution ranged from ≈400 to >5000 base pairs.

Suitable films of hydrated nonoriented DDD (NaDNA) with $\Gamma = 8$, 13 (14), and 20 were obtained by dissolving ≈0.7 mg of dry DDD (NaDNA) in ≈60−70 mg of water, by transferring the aqueous solution on a AgCl disk, and by keeping the aqueous solution and disk in a desiccator for several days at relative humidities of 80.3, 84.3, and 92.5% (obtainable with saturated $(NH_4)_2SO_4$, KCl, and KNO_3 solution). The hydrated films were thereafter quickly covered with a second AgCl disk, the two disks were taped, and the sample was positioned in a sample holder made of aluminum for the cryostat. Special care was taken to avoid orientation of the films, and the method of preparation ensures nonoriented films.

The temperature of the sample holder and the taped AgCl windows was regulated with a thermocontroller (AP Paar, model TTK-HC) and remained constant within ±0.1°. Slow-cooled films were obtained by cooling at a rate of 2 K min^{-1}. Fast-cooled films were obtained for generating a nonequilibrium distribution of conformer substates, and the sample and the sample holder were quenched to ≈160 K into the glassy state while inside the cryostat, by forcing liquid N_2 through the cooling tubes of the sample holder. This results in an average cooling rate of ≈90 (or ≈60) K min^{-1}. A pressure of ≈600 mbar of N_2 was maintained in the cryostat during the whole experiment in order to avoid dehydration of the films.

FT-IR Spectroscopy. IR spectra were recorded in transmission mode on Biorad's FTS-45 model at 4 cm^{-1} resolution by coadding 64 scans (UDR1; DTGS detector; zero-filling factor 2; low pass filter at 1.12 kHz; triangular apodization). The collection time of 150 s constitutes the time resolution. The Γ values of the films were determined from band area ratios of the OH stretching vibration and the antisymmetric stretching vibration of the ionic PO_2^- group.[58,59] First, IR spectra of the DDD (NaDNA) films were recorded on slow cooling at 2 K min^{-1} at selected temperatures between 290 and 180 K. IR spectra of the films fast-cooled to 160−170 K at a rate of ≈90 (or ≈60) K min^{-1} were recorded thereafter isothermally at 180, 200, and 220 K, and spectral changes caused by CSs interconversion were followed as a function of time in the form of difference spectra. The absence of dehydration or irreversible spectral changes was confirmed by comparing IR spectra recorded at 290 K before and after the low-temperature experiments, and in this way, changes in concentration and/or thickness of the films were ruled out. This is an important aspect for estimation of B_I/B_{II} population ratios which requires constant

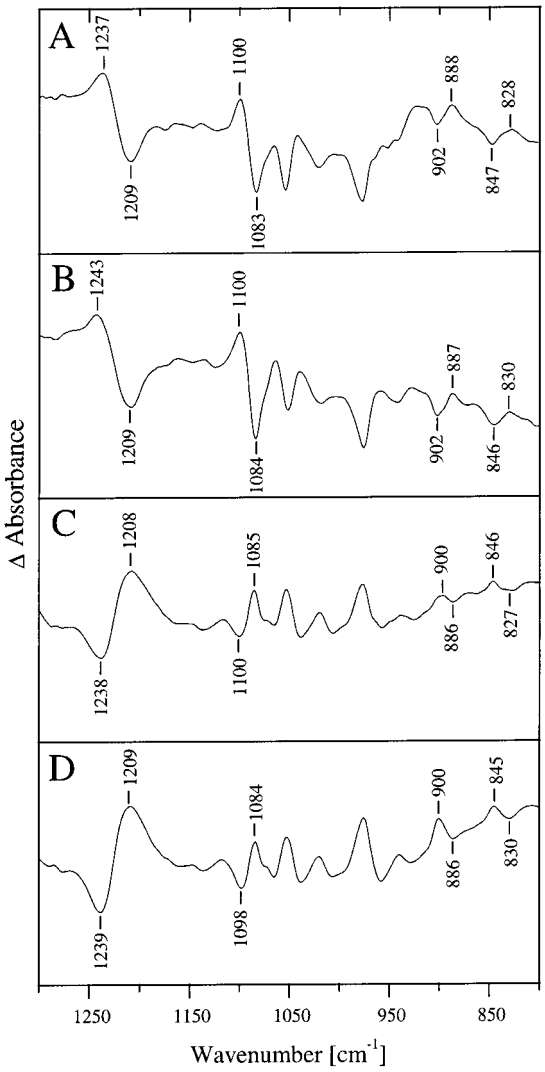

Figure 1. Comparison of difference curves (from 1300 to 800 cm^{-1}) obtained on isothermal annealing (A and B), with those obtained from spectra recorded at different temperatures (C and D). (A) the difference curve obtained by subtracting the spectrum of a quenched d(CGCGAATTCGCG)$_2$ film ($\Gamma = 13$) recorded at 200 K after 4 min from that recorded after 25 min; (B) the corresponding difference curve from NaDNA from salmon testes ($\Gamma = 12$, 200 K, 26−4 min); (C) the difference curve from a d(CGCGAATTCGCG)$_2$ film ($\Gamma = 14$) obtained by subtracting the spectrum recorded at 290 K from that at 270 K; (D) the corresponding difference curve from NaDNA from salmon testes ($\Gamma \approx 20$, 270−290 K). Note the mirror image between A and C on the one hand and B and D on the other (from ref 10).

($B_I + B_{II}$) concentration and film thickness. The spectra are displayed in the figures on the same ordinate scale. Vertical bars indicate the ordinate scale in absorbance units. Second derivative curves are shown inverted. For details on treatment of the IR spectra and of curve resolution, ref 13 should be consulted.

Results and Discussion

Incentive for this study was our unexpected observation of reversal of CSs transitions; that is, B_{II} converts to B_I on cooling from ambient temperature, and B_I converts to B_{II} on isothermal relaxation of fast-cooled films at 200 K.[7−13] This is shown in Figure 1 where we compare the isothermal difference curves obtained with the dodecamer and with B-DNA from salmon testes with difference curves obtained from spectra recorded at two different temperatures. Curves A and B are the difference

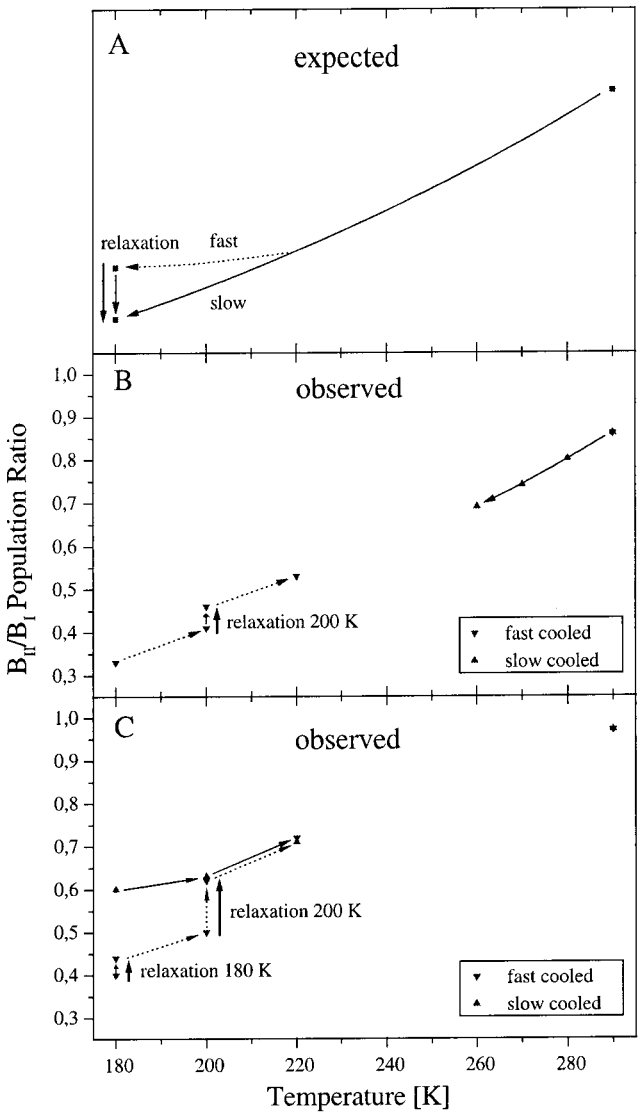

Figure 2. Effect of cooling rate in the form of B_{II}/B_I population ratio versus temperature plots. Plot A visualizes the expected behavior; that is, the B_{II}/B_I population ratio is higher in the fast-cooled film (broken) than in the slow-cooled film (solid), and consequently, on isothermal relaxation, B_{II} converts into B_I. Plots B and C show the experimentally observed behavior for two hydrated films of the $d(CGCGAATTCGCG)_2$ dodecamer with $\Gamma = 14$ (B) and 13 (C). Solid triangles are for data points obtained on slow cooling, whereas inverted triangles are for data points obtained on fast cooling at ≈60 (B) or ≈90 (C) K min^{-1}. For both B and C, the B_{II}/B_I population ratio is lower in the fast-cooled film than in the slow-cooled film, and therefore, B_I converts into B_{II} on isothermal relaxation at 180 and 200 K. The dodecamer was purified for B by precipitation from cold ethanol and for C by HPSF.

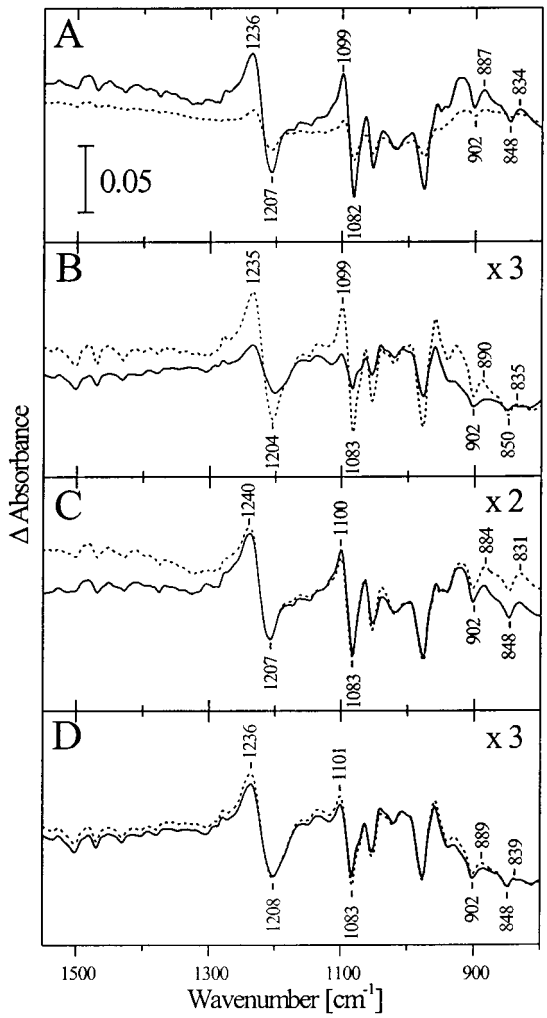

Figure 3. Relaxation of the fast-cooled film of the hydrated $d(CGCGAATTCGCG)_2$ dodecamer film, with $\Gamma = 13$ (for plot C of Figure 2) compared with that of the same film but cooled slowly in the form of difference curves (from 1550 to 800 cm^{-1}). Plot A compares relaxation effects at 180 K: the solid-line difference curve is obtained by subtracting the spectrum of the fast-cooled film from that of the slow-cooled film, both spectra recorded at 180 K after 1 min; the dotted-line difference curve is obtained by subtracting the spectrum of the fast-cooled film recorded at 180 K after 1 min from that of the same film recorded after 120 min. Plot B compares relaxation effects on heating from 180 to 200 K: the solid difference curve is for the slow-cooled film, obtained by subtracting the spectrum recorded at 180 K (after 7 min) from that at 200 K (after 1 min); the dotted difference curve is for the fast-cooled film, obtained by subtracting the spectrum recorded at 180 K after 120 min from that at 200 K after 1 min. Plot C compares relaxation effects at 200 K: the solid difference curve is obtained by subtracting the spectrum of the fast-cooled film from that of the slow-cooled film, both spectra recorded at 200 K after 1 min; the dotted difference curve is obtained by subtracting the spectrum of the fast-cooled film recorded at 200 K after 1 min from that of the same film recorded after 80 min. Plot D compares relaxation effects on heating from 200 to 220 K: the solid difference curve is for the slow-cooled film, obtained by subtracting the spectrum recorded at 200 K (after 7 min) from that at 220 K (after 1 min); the dotted difference curve is for the fast-cooled film, obtained by subtracting the spectrum recorded at 200 K after 80 min from that at 220 K after 1 min. The difference curves are drawn on the same scale, multiplied by the factors in the figure.

curves obtained on isothermal CS interconversion at 200 K with DDD and B-DNA from salmon testes ($\Gamma = 13$ and 12). Curves C and D are the 270−290 K difference curves obtained with DDD and B-DNA from salmon testes ($\Gamma = 14$ and 20). The spectral region is shown only from 1300 to 800 cm^{-1}, because outside of this region pronounced changes in the band shapes of the water bands occur with change in temperature which leads to sloping in the difference spectra. The comparison in Figure 1 demonstrates that curves C and D are on the whole the mirror image of curves A and B and that the positive and negative band positions are very similar. This indicates, first, that on cooling from 290 to 270 K the opposite CSs interconversion occurs than on isothermal relaxation at 200 K. Figure 1 further demonstrates that the same spectral changes occur in the synthetic DDD and in polymeric B-DNA from salmon testes. By comparison with the IR spectrum of a single crystal of DDD (from ref 40) and careful curve resolution, we could assign these spectral changes to the transition between B-DNA's conformer substates, where B_{II} converts into B_I on cooling from 290 to

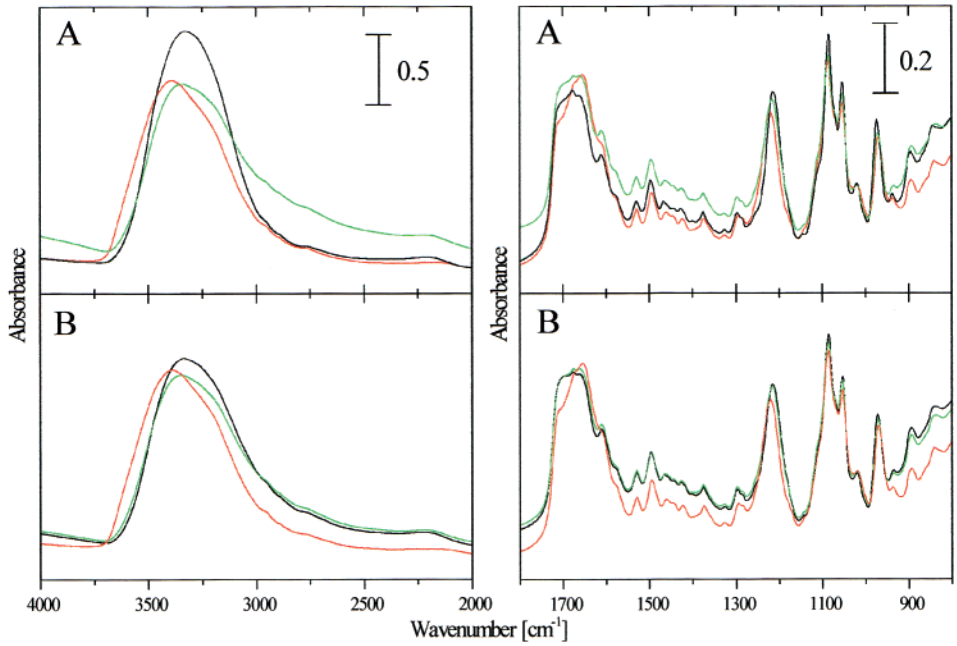

Figure 4. Effects of cooling rate and of relaxation as seen in IR spectra of the hydrated d(CGCGAATTCGCG)$_2$ dodecamer film, with $\Gamma = 13$ (for plot C of Figure 2). The spectra show the OH stretching band region (from 4000 to 2000 cm^{-1}, drawn on the same scale) and, on an enlarged scale, the spectral region from 1800 to 800 cm^{-1}. Plot A compares spectra of the fast-cooled film recorded at 180 K after 1 min (black) and at 220 K after 35 min (green) with that of the equilibrated film recorded at 290 K (red). Plot B compares spectra of the same film but cooled slowly and recorded at 180 K after 1 min (black) and at 220 K after 20 min (green) with that of the film recorded at 290 K (red). Note the change of the OH stretching band profile of the fast-cooled sample on low-temperature relaxation (A, black to green) and its absence in the slow-cooled sample (B).

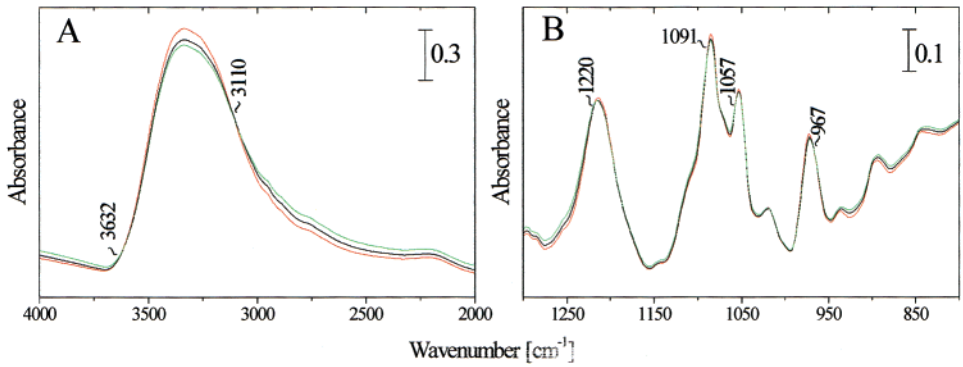

Figure 5. Relaxation of the fast-cooled hydrated d(CGCGAATTCGCG)$_2$ dodecamer film ($\Gamma = 13$) at 200 K as seen in the IR spectra. The spectra are drawn on the same scale, and they show the OH stretching band region (from 4000 to 2000 cm^{-1}) and, on an enlarged scale, the spectral region from 1300 to 800 cm^{-1}. The spectra were recorded after 1 (red), 10 (black), and 80 (green) min, respectively. Note the isobestic points which are indicated by the wavenumber positions.

260 K and B_I converts into B_{II} at 200 K on isothermal relaxation of a quenched film.[8−13]

This paper is structured as follows. We first show for the synthetic DDD with $\Gamma = 13$ (or 14) the effect of cooling rate on the low-temperature dynamics, i.e., the B_I and B_{II} conformer substate interconversion derived from the IR spectroscopic features (Figures 2−5). DDD is solely in the B-form,[31] independent of its hydration, and thus, problems with formation of A-DNA at low water activity are avoided. For this hydration, restructuring of hydration shells rules the low-temperature dynamics and the B_I to B_{II} CSs interconversion. In a next step, we compare the low-temperature dynamics of the DDD films with $\Gamma = 13$ (or 14) with that of a film with $\Gamma = 8$ (Figures 6 and 7). In the latter case, the B_I/B_{II} interconversion is not affected by changes in the cooling rate. Therefore, the effect of cooling rate in DDD films with $\Gamma = 13$ must be caused by the additional water molecules. Finally, we show that highly polymeric native B-DNA from salmon testes shows the same effects as the synthetic dodecamer (Figure 8). For native B-DNA, formation of A-DNA on reducing the water activity interferes, and therefore, the experimental evidence for the restructuring of hydration shells has to be less extensive. Even so, the comparison indicates that our conclusions seem to be general and not restricted to the synthetic oligonucleotide.

Isothermal $B_I \rightarrow B_{II}$ Relaxation in Hydrated DDD Films with $\Gamma = 13$ (or 14). Here we show that the reversal in conformer substate interconversion is caused by two distinct processes occurring on cooling, a comparatively slow one involving restructuring of hydration shells and a faster one which is the conformer substate interconversion. The key for separating these two processes is to compare B_{II}/B_I population ratios obtained on fast cooling with those of slow-cooled films. References 8, 11, and 13 should be consulted for details on determining B_{II}/B_I population ratios via curve resolution of IR spectra.

Figure 2 shows three plots of B_{II}/B_I population ratios versus temperature and the comparison of the effects of fast-cooling with those of slow-cooling. Plot A (top) demonstrates the

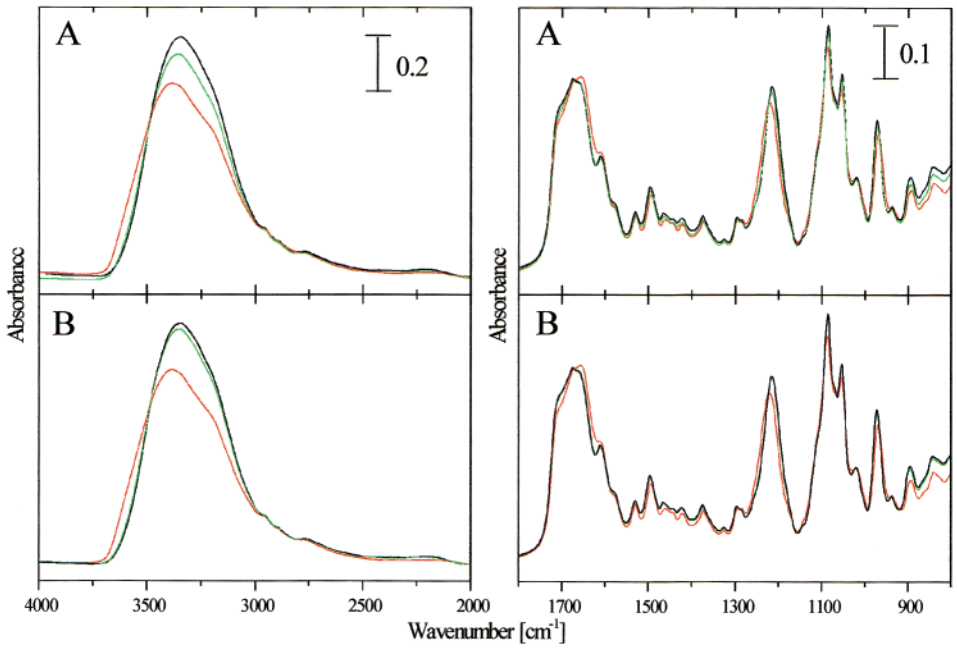

Figure 6. Effects of cooling rate and of relaxation as seen in experimental spectra of the hydrated d(CGCGAATTCGCG)$_2$ dodecamer film, with $\Gamma = 8$. The spectra show the OH stretching band region (from 4000 to 2000 cm^{-1}, drawn on the same scale) and, on an enlarged scale, the spectral region from 1800 to 800 cm^{-1}. Plot A compares spectra of the fast-cooled film recorded at 180 K after 1 min (black) and at 220 K after 35 min (green), with that of the equilibrated film recorded at 290 K (red). Plot B compares spectra of the same film but cooled slowly and recorded at 180 K after 1 min (black) and at 220 K after 20 min (green) with that of the film recorded at 290 K (red).

expected behavior; that is, a fast-cooled film departs at some temperature (220 K in plot A) from the equilibrium line obtained on slow-cooling. Therefore, isothermal relaxation at 180 K (indicated by the arrow) would also occur via transition of $B_{II} \rightarrow B_I$. This "expected" behavior apparently does not explain the reversal of CSs interconversion pointed out in Figure 1.

Plots B and C demonstrate the experimentally observed behavior, and they were obtained with two films of hydrated DDD with $\Gamma = 14$ (B) and 13 (C). DDD used for plots B and C was purified differently. Plots B and C differ mainly with respect to the amount of relaxation at 180 and 200 K, but the trend in terms of reversal of CSs interconversion is the same. Triangles are for data points obtained on slow cooling either in steps (B) or at 2 K min^{-1} (C), whereas inverted triangles are for data points obtained on fast cooling at an average rate of $\approx$60 (B) and $\approx$90 (C) K min^{-1}. The data points at high temperatures (290−260 K for B and 290 K for C) were obtained by curve resolution of infrared spectra of equilibrated films, and the B_{II}/B_I population ratio obtained for 290 K is similar for both films (0.86 for B and 0.97 for C). Data points of slow-cooled films obtained from IR spectra recorded at 180, 200, and 220 K also seem to be for (nearly) equilibrated films because these films do not show evidence for isothermal relaxation.

However, the data points of fast-cooled films obtained for 180 and 200 K are for nonequilibrated films, because these films show relaxation effects as shown in Figure 1. Plots B and C reflect the reversal in CSs interconversion seen in Figure 1 in the form of difference curves, in that the B_{II}/B_I CS population ratio is *lower* for the fast-cooled film than for the slow-cooled film, and therefore, B_I converts into B_{II} on isothermal relaxation at 180 (C) and 200 K (B and C), as indicated by the arrows. In plot C, the B_{II}/B_I population ratio at 200 K is 0.63 for the slow-cooled film and 0.62 for the fast-cooled film after relaxation for 80 min, and therefore, the latter had approached equilibrium. The difference in the amount of relaxation between plots B and C is attributed to differences in cooling rate and possibly to variations in purifying DDD. We believe that the samples deviate on fast-cooling from the equilibrium line around $\approx$240−220 K because isothermal relaxation effects at 220 K are minor on fast cooling to $\approx$180 K and subsequent heating to 220 K. IR spectra were not recorded between 260−220 K (Figure 2B) and 290−220 K (Figure 2C) in order to reduce the length of the experiment to a reasonable time, and thus, data points are not available.

The B_{II}/B_I population ratios in plots B and C of Figure 2 obtained by curve resolution are further consistent with the spectral changes seen in the form of difference curves. Estimates for changes in B_{II}/B_I populatio ratios obtained from difference curves (Figure 3) are included in Figure 2 in the form of dotted lines. Figure 3 shows difference curves obtained from spectra recorded with the DDD film used for plot C of Figure 2. Plot A compares relaxation effects at 180 K: the solid-line difference curve is obtained by subtracting the spectrum of the fast-cooled film from that of the slow-cooled film, with both spectra recorded at 180 K after 1 min, and thus, it represents the difference in B_{II}/B_I population ratio between fast-cooling and slow-cooling. The dotted-line difference curve in A is obtained by subtracting the spectrum of the fast-cooled film recorded at 180 K after 1 min from that of the same film recorded after 120 min, and it represents the amount of $B_I \rightarrow B_{II}$ conformer interconversion. The comparison between the two difference curves is done best with the separated characteristic feature from the antisymmetric stretching vibration of the ionic phosphate group, ν_{as} PO_2^-, between 1200 and 1250 cm^{-1} where the positive feature centered at 1236 cm^{-1} is from B_{II} and the negative one at 1207 cm^{-1} is from B_I.[8−13] This comparison shows that isothermal relaxation of the fast cooled film (dotted) is only about one-third of the entire difference in Δ(absorbance) between the fast-cooled and slow-cooled film (solid). This is qualitatively consistent with the data points in plot C of Figure 2 where the B_{II}/B_I population ratio of the fast-cooled film increases on isothermal relaxation at 180 K from 0.40 to 0.44, whereas the B_{II}/B_I population ratio of the slow-cooled film is at 0.60.

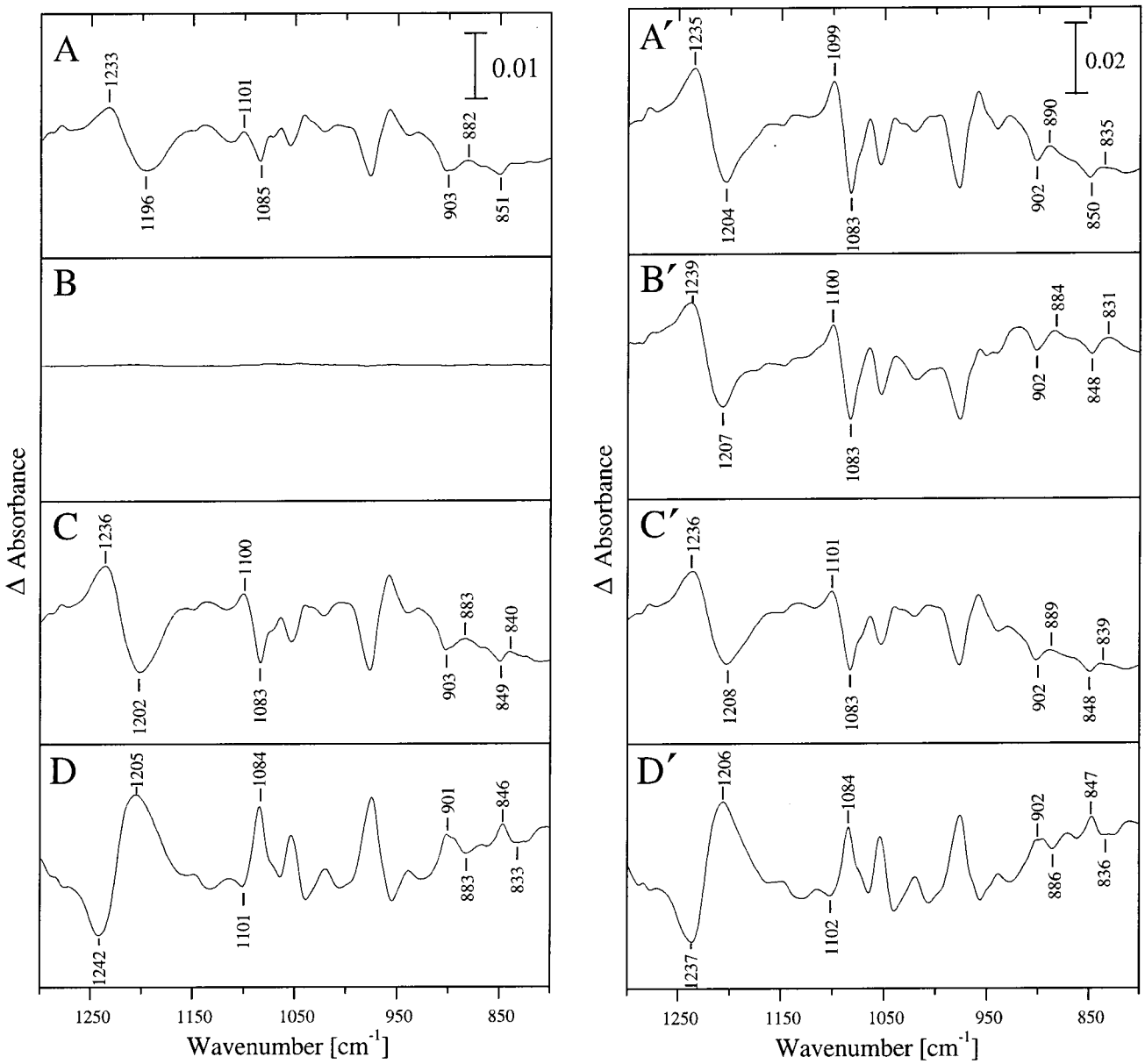

Figure 7. Comparison of the effects of temperature and of isothermal relaxation in the hydrated d(CGCGAATTCGCG)$_2$ dodecamer film, with $\Gamma = 8$ (left), with that in the film with $\Gamma = 13$ (right) as seen in the form of difference curves obtained from spectra after fast cooling. Difference curves A and A′ were obtained by subtracting the spectra recorded at 180 K (for A after 13 min and for A′ after 120 min) from those recorded at 200 K after 1 min. Difference curves B and B′ were obtained by subtracting spectra recorded at 200 K after 1 min from those recorded after 15 min. Difference curves C and C′ were obtained by subtracting the spectra recorded at 200 K (for C after 15 min, for C′ after 80 min) from those recorded at 220 K after 1 min. For comparison, the difference curves D and D′ are also shown which were obtained by subtracting spectra recorded at 290 K from those at 270 K. Note the similarity of spectral changes on heating, and the absence of isothermal relaxation in B.

In the same manner, plot B of Figure 3 compares relaxation effects on heating from 180 to 200 K: the solid difference curve is for the slow-cooled film, obtained by subtracting the spectrum recorded at 180 K (after 7 min) from that recorded at 200 K (after 1 min); the dotted difference curve is for the fast-cooled film, obtained by subtracting the spectrum recorded at 180 K after 120 min from that recorded at 200 K after 1 min. In the spectral region of ν_{as} PO_2^-, the Δ(absorbance) of the solid difference curve is about one-third of the dotted difference curve, and this is consistent with the changes in the B_{II}/B_I population ratio on heating from 180 to 200 K (Figure 2, plot C: B_{II}/B_I of the slow-cooled film is 0.60 at 180 K and 0.63 at 200 K; B_{II}/B_I of the fast-cooled film is 0.44 at 180 K after 120 min and 0.50 at 200 K after 1 min).

Plot C of Figure 3 compares relaxation effects at 200 K: the solid difference curve is obtained by subtracting the spectrum of the fast-cooled film from that of the slow-cooled film, with both spectra recorded at 200 K after 1 min; the dotted difference curve is obtained by subtracting the spectrum of the fast-cooled film recorded at 200 K after 1 min from that of the same film recorded after 80 min. Both difference curves are nearly identical, and therefore, the fast-cooled film approaches after 80 min the B_{II}/B_I population ratio of the slow-cooled film. This again is consistent with the results from curve resolution as shown in plot C of Figure 2 (at 200 K: the B_{II}/B_I ratio of the slow-cooled film is 0.63, and of the fast-cooled film, it is 0.62 after 80 min). Finally, plot D of Figure 3 compares relaxation effects on heating from 200 to 220 K: the solid difference curve is for the slow-cooled film, obtained by subtracting the spectrum recorded at 200 K (after 7 min) from that at 220 K (after 1 min); the dotted difference curve is for the fast-cooled film, obtained by subtracting the spectrum recorded at 200 K after

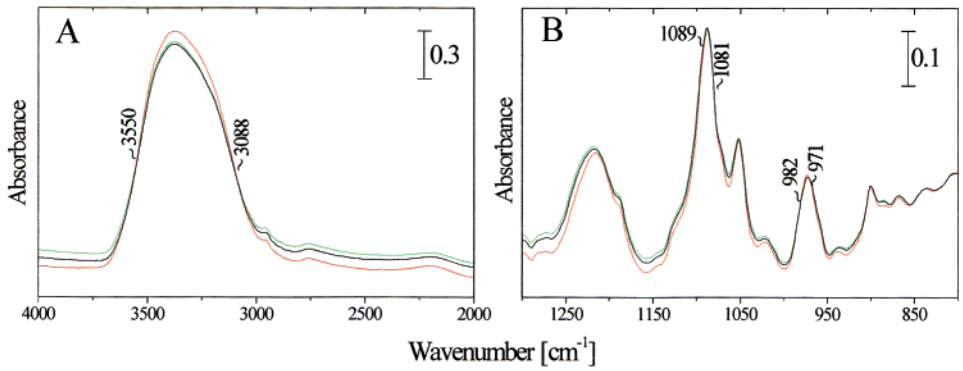

Figure 8. Relaxation of a fast-cooled hydrated DNA film from salmon testes, with $\Gamma = 12$, at 200 K as seen in the experimental spectra. The spectra are drawn on the same scale, and they show the OH stretching band region (from 4000 to 2000 cm^{-1}) and, on an enlarged scale, the spectral region from 1300 to 800 cm^{-1}. The spectra were recorded after 1 (red), 25 (black), and 112 (green) min, respectively. Note the isobestic points which are indicated by the wavenumber positions.

80 min from that at 220 K after 1 min. Similarity of these difference curves is consistent with our result from curve resolution in that the fast-cooled film approaches on isothermal relaxation at 200 K the B_{II}/B_I equilibrium population ratio of the slow-cooled film (see plot C of Figure 2). On further heating from 200 to 220 K, the change in the B_{II}/B_I ratio is similar for both films (the B_{II}/B_I ratio of the slow-cooled film increases on heating from 200 to 220 K from 0.63 to 0.71, and that of the fast-cooled film increases from 0.62 to 0.72). We emphasize that for slow-cooled films isothermal relaxation effects either at 180 or 200 K are negligible and, thus, that isothermal difference curves are a straight line on the Δ(absorbance) scale of Figure 3. This is consistent with equilibration on slow cooling.

Restructuring of Hydration Shells. We next show that the unexpected reversal in B-DNA's $B_I \leftrightarrow B_{II}$ interconversion can be attributed to restructuring of their hydration shells. Figure 4 shows the effects of cooling rate and of relaxation as seen in IR spectra of the hydrated DDD film, with $\Gamma = 13$, which had been used for plot C of Figure 2. The spectra show the OH stretching band region (from 4000 to 2000 cm^{-1}) and, on an enlarged scale, the spectral region from 1800 to 800 cm^{-1}. Plot A compares spectra of the fast-cooled film recorded at 180 K after 1 min (black) and at 220 K after 35 min (green) with that of the equilibrated film recorded at 290 K (red). The major change in the OH stretching band region of the fast-cooled film recorded at 180 K (black) is enhanced intensity which is attributed to increasing absorptivity.[60] However, pronounced spectral changes occur on relaxation and heating to 220 K in that the OH stretching band gains considerable intensity at low wavenumbers and the whole spectrum is shifted upward. We attribute the first effect to enhanced hydrogen-bond interaction[7−13] and the second to enhanced absorptivity. Plot B compares spectra of the same film but cooled slowly and recorded at 180 K after 1 min (black) and at 220 K after 20 min (green) with that of the film recorded at 290 K (red). This comparison shows that pronounced spectral changes occur already on slow cooling to 180 K and that only minor effects are observable on heating to 220 K which are attributable to changes in absorptivity. These spectral effects of the slow-cooled film at 180 K are very similar to those of the fast-cooled film after relaxation and heating to 220 K.

We emphasize that the spectral changes observable in the OH stretching band region of Figure 4 (and the following Figure 6) are not caused by formation of ice. Formation of small amounts of ice is recognizable in the experimental spectra by the peak centered at ≈3240 cm^{-1} superimposed on the broad feature of unfreezable water[59] and, even more clearly, in isothermal difference curves by formation of a sharp feature centered at ≈3120 cm^{-1}.[10] Dodecamer films with $\Gamma = 13$ contain only unfreezable water, and it requires higher Γ values until water becomes partly freezable.[8,10,59]

We attribute these spectral changes in the OH stretching band region to restructuring of the hydration shells of B-DNA's B_I and B_{II} CSs toward increased hydrogen-bond interaction. This restructuring is a comparatively slow process and thus can be avoided by fast cooling at ≈90 (or ≈60) K min^{-1}. In other words, the high-temperature hydration shells are frozen-in, and it requires either isothermal relaxation at sufficiently high temperature (e.g., at 200 K) or heating to 220 K for their equilibration. However, in films cooled slowly to 180 K at 2 K min^{-1}, restructuring of hydration shells occurs during cooling, and the structural state observable at 180 K approaches that of the equilibrated low-temperature hydration shells.

In this scenario, comparatively slow restructuring of hydrations shells is the cause for our unexpected findings of reversal of B-DNA's $B_{II} \rightarrow B_I$ conformer substates interconversion in fast-cooled films (see Figure 1 and Figure 2, B and C). Once there is either sufficient time on isothermal relaxation (at 200 or 180 K) or the temperature is high enough for restructuring of hydration shells, hydrogen bonding increases as evidenced by the pronounced shift of the OH stretching band to lower wavenumbers, and B_{II} becomes stabilized relative to B_I. This is observable in the cooling experiments where the B_{II}/B_I population ratio is higher on slow-cooling than on fast-cooling because only on slow cooling restructuring of hydration shells can occur toward increased hydrogen bonding (Figures 2 and 4). It also holds for the isothermal experiments with fast-cooled films where the isothermal $B_I \rightarrow B_{II}$ relaxation observable at 180 and 220 K (Figure 2) is accompanied by increased hydrogen bond interaction as shown in Figure 5.

Figure 5 shows isothermal relaxation effects of the fast-cooled DDD film, with $\Gamma = 13$, at 200 K as seen in the infrared spectra. For clarity, only three spectra are shown which were recorded after 1 (red), 10 (black), and 80 (green) min, and five additional infrared spectra recorded between are not included in the figure. The spectra show the OH stretching band region from 4000 to 2000 cm^{-1} and, on an enlarged scale, the spectral region from 1300 to 800 cm^{-1}. Spectral changes occur in the same manner as those shown in Figure 4A on heating from 180 to 220 K, although to a minor extent, in that the OH stretching band gains intensity at low wavenumbers and that the whole spectrum shifts to higher absorbance. These spectral changes become apparent in difference curves in the form of a positive feature centered

at ≈2840 cm^{-1} and of two negative features at ≈3490 and ≈3285 cm^{-1} (see Figure 1 in refs 8 and 10).

We further indicate in Figure 5 by wavenumber positions where "isobestic points" occur, that is, where at the given wavenumber the series of infrared spectra (including the 5 spectra not shown) cross and the absorbance is constant. An isobestic point may mean that, for constant concentration, interconversion between two species occurs.[61] For Figure 5, these two species are the B_I and B_{II} CSs of B-DNA. The observation of isobestic points in the OH stretching band region indicates that on isothermal $B_I \rightarrow B_{II}$ transition, also changes in hydration shells of the conformer substates occur. Because their time scales are comparatively slow, as evidenced by Figure 4, we conclude that on isothermal relaxation first restructuring of hydration shells toward increased hydrogen-bond interaction must occur which then drives the $B_I \rightarrow B_{II}$ transition toward equilibrium. The average relaxation time (τ_a) of this process is ≈10 min at 200 K.[9,13] The isobestic points at ≈3110 and ≈3632 cm^{-1} are not observable in spectra recorded at different temperatures between 180 and 220 K because in these spectra additional changes in band profile with temperature occur.

One of the reviewers suggested to prove that first hydration shells and then the B_I/B_{II} ratio change, by comparing the kinetics of the two processes: this could be done in principle for fast-cooled films by plotting the B_I/B_{II} ratio and change of hydration shell structure as a function of annealing time at 200 K. However, this is at present not possible with our comparatively slow IR spectroscopic detection of structural changes. In our view, slow change of hydration shells is followed by much more rapid $B_I \rightarrow B_{II}$ transition (based on the comparison with the behavior of fast-cooled films with $\Gamma = 8$ and 6), and we cannot yet separate these two processes.

Our interpretation of the unexpected $B_I \rightarrow B_{II}$ relaxation in fast-cooled films in terms of slowing down of hydration shell dynamics around ≈240−220 K is consistent with NMR spectral studies of Kuntz et al.[62] They observed that, on cooling to 238 K, "the DNA decreases, but does not completely eliminate, the mobility of adjacent water molecules" and that 11 water molecules per nucleotide are affected in this way.[63]

Absence of Isothermal $B_I \rightarrow B_{II}$ Relaxation in Hydrated DDD Films with $\Gamma = 8$. Further support for the above scenario comes from the comparison of the spectra depicted in Figure 4 for a DDD film with $\Gamma = 13$, with those of a DDD film with $\Gamma = 8$. In Figure 6, the effects of cooling rate and of relaxation on the IR spectra of a DDD film with $\Gamma = 8$ are presented in the same manner as those in Figure 4 (for DDD with $\Gamma = 13$). Plot A compares spectra of the fast-cooled film recorded at 180 K after 1 min (black) and at 220 K after 35 min (green) with that of the equilibrated film recorded at 290 K (red). Contrary to Figure 4, the effects of relaxation and heating from 180 to 220 K (black versus green) are minor, and neither increased intensity of the OH stretching band at lower wavenumbers nor pronounced upward shift of the whole spectrum are observable. Figure 6B compares spectra of the same film but cooled slowly and recorded at 180 K after 1 min (black) and at 220 K after 20 min (green) with that of the film recorded at 290 K (red). Only the increased intensity of the spectra recorded at 180 and 220 occurs which is attributed to increased absorptivity. Thus, the pronounced spectral changes observable in Figure 4B and attributed to restructuring of hydration shells are absent in Figure 6B.

We thus conclude that restructuring of the hydration shells of B_I and B_{II} requires more than eight water molecules per nucleotide, and it involves the additional water molecules present in a film with $\Gamma = 13$. In additional studies of DDD films with $\Gamma = 6$ and 20, we observed that spectra from films with $\Gamma = 6$ showed the same behavior as those with $\Gamma = 8$, and spectra from films with $\Gamma = 20$ are similar to those with $\Gamma = 13$ except for formation of some ice.[10]

We have argued that restructuring of hydration shells of B_I and B_{II} rules their interconversion. Therefore, the absence of such slow restructuring shown in Figure 6 for the film with $\Gamma = 8$ should also influence the interconversion of the conformer substates of B-DNA. This is indeed the case, and it is demonstrated by Figure 7. In this figure, we compare for fast-cooled films the effects of temperature and of isothermal relaxation in the hydrated DDD film with $\Gamma = 8$ (left) with that in the film with $\Gamma = 13$ (right) in form of difference curves. Difference curves A and A′ were obtained by subtracting the spectra recorded at 180 K from those recorded at 200 K after 1 min, and they display similar spectral changes on heating.

Difference curves B and B′ were obtained by subtracting spectra recorded at 200 K after 1 min from those recorded after 15 min and, thus, represent the spectral changes on isothermal relaxation at 200 K. Spectral changes are negligible for B in comparison to B′. This is consistent with our notion that slow restructuring of hydration shells occurs only for B′, the DDD film with $\Gamma = 13$, and that it drives the $B_I \rightarrow B_{II}$ transition. Comparable restructuring of hydration shell does not occur for B where the dodecamer film has a Γ value of 8 (see Figure 6). Therefore, in the absence of slow hydration shell restructuring, the isothermal $B_I \rightarrow B_{II}$ transition is much faster and cannot be registered within the time scale of our infrared experiment. Difference curves C and C′ display similar spectral changes on heating from 200 to 220 K. Difference curves D and D′ display for comparison the spectral changes on cooling from 290 to 270.

Isothermal $B_I \rightarrow B_{II}$ Relaxation in Native Hydrated Polymeric B-DNA. We next extend our study to native highly polymeric B-DNA from salmon testes. It is not possible to investigate restructuring of hydration shells in the same manner described above for the synthetic dodecamer because, for complete conversion of A-DNA into B-DNA, ≈20 water molecules per nucleotide are required which partly freeze on cooling.[8,10,59] Films with $\Gamma = 12$ consist of unfreezable water, but these are a mixture of ≈30% B-DNA and 70% A-DNA.[4,23,56,64] Reliable curve resolution of infrared spectra obtained from the latter films is not possible because the bands from A-DNA interfere.

We recently reported that the overall appearance of the dodecamer's difference curves obtained on isothermal relaxation at 200 K and that of the one obtained with B-DNA from salmon testes are remarkably similar.[8−10,12] Figure 1 further indicates that the behavior of B-DNA from salmon testes is comparable with that of DDD in that both show similar reversal of conformer substate interconversion.

Figure 8 shows isothermal relaxation effects of the fast-cooled DNA film from salmon testes, with $\Gamma = 12$, at 200 K as seen in the infrared spectra. The spectra show the OH stretching band region from 4000 to 2000 cm^{-1} and, on an enlarged scale, the spectral region from 1300 to 800 cm^{-1}. For clarity, only three spectra are shown which were recorded after 1 (red), 25 (black), and 112 (green) min, and six additional infrared spectra recorded between are not included in the Figure. Spectral changes occur in the same manner as those shown for the dodecamer in Figure 5, in that the OH stretching band gains intensity at low wavenumbers and that the whole spectrum shifts upward. In accordance with the study of the dodecamer (Figure 5), we

attribute these spectral changes also to restructuring of hydration shells of the B_I and B_{II} conformer substate on $B_I \rightarrow B_{II}$ interconversion. Isobestic points were determined by including the six spectra not shown for clarity. These are marked by the wavenumber positions and they indicate conversion of one species into another one. A-DNA is not involved in isothermal relaxation because A-DNA marker bands are absent in difference curves, for example the sharp characteristic band at 1188 cm^{-1}.[65]

The upward shift of spectra observable in Figures 4-8 at low temperatures for slow-cooled films and for fast-cooled films after relaxation and heating to 220 K requires discussion. Careful studies of the absorptivity of hexagonal ice in the range of 4000−30 cm^{-1} by Bertie et al.[60] have shown that "the fundamental bands are underlain by a relatively strong absorption that is caused by overtones and combinations. Much of this absorption has no recognizable features, and detailed assignments cannot be made". In the same manner, the upward shift of spectra observable in Figures 4-8 is attributed to increased absorptivity of the unfreezable water molecules involved in restructuring of the hydration shells. We consider an alternative explanation in terms of increasing stray light or by the Christiansen effect unlikely as follows. The latter type of distortion of infrared spectra is observed only for absorption bands with rapidly changing refractive indices, and it leads to asymmetry and even shift of band maxima. However, isobestic points observable in the OH stretching band region of Figures 5 and 8 are consistent with interconversion of two species of overall constant concentration but not with increasing stray light or distortion of spectra by the Christiansen effect. Our interpretation of the apparent increase in absorptivity attributed to restructuring of hydration shells on $B_I \rightarrow B_{II}$ conversion is further consistent with our observation that it ceases in isothermal studies of fast-cooled films at 200 K (cf. Figures 5 and 8) once equilibrium had been attained and B_I does not convert anymore to B_{II}.

Why Is the B_{II}/B_I Population Ratio in Fast-Cooled, Nonequilibrated Films with $\Gamma = 13$ (14) *Below* the B_{II}/B_I Equilibrium Value? Here we can only speculate, but the conjecture must involve thermodynamic arguments in addition to kinetics because otherwise we would observe the "expected" situation depicted in Figure 2a. We recently observed on careful curve resolution of hydrated DDD films that the fwhh of the symmetric stretching vibration (υ_s) of the ionic PO_2^- group is much larger for B_{II} than for B_I.[8,11,13] Enhanced fwhh of the B_{II} band indicates a larger distribution of oscillators for υ_s of B_{II} than that of B_I, and this could be caused by a broader distribution of backbone torsion angles in B_{II} than in B_I.[13] Thus, it is conceivable that on cooling DDD the broader distribution of torsion angles in B_{II} and their slight changes with temperature require for the B_{II} hydration shell larger restructuring for optimal interaction than for the B_I hydration shell. This restructuring could be too slow on fast-cooling films with $\Gamma = 13$ (14), and therefore, B_{II} could be less well stabilized by hydrogen-bond interaction with its hydration shell than B_I once the hydration shells have become immobilized. This in turn can lead to further $B_{II} \rightarrow B_I$ conversion, beyond the equilibrium value. Our conjecture is consistent with our observation that isothermal relaxation toward equilibrium via $B_I \rightarrow B_{II}$ conversion is accompanied by enhanced hydrogen-bond interaction of the B_{II} substate with its hydration shell (see Figure 1 in ref 8 and Figure 2 in ref 13).

Relevance for the "200 K Glass-Like Transition" in Biomolecules and the Low-Temperature Limit of their Functions. The low-temperature dynamics of biomolecules, mainly of proteins, has been studied by various techniques, and the onset of dynamics was observed at ≈180−200 K.[66−81] This has been called the "200 K glass-like transition".[81] In DSC heating curves of fast-cooled samples, the onset of dynamics was observed at ≈150−170 K.[82−86] Sokolov et al.[55] recently studied the glassy dynamics in DNA and discussed whether it is "ruled by water of hydration". They used hydrated oriented LiDNA fibers in the B-form, with $\Gamma \approx 15$, and applied inelastic neutron scattering spectroscopy for measurements of atomic motion which give directly density fluctuations. Their analysis revealed two temperature ranges at which the dynamics of DNA exhibits qualitative changes. The first is at ≈180−200 K where the intensity increase "reflects strongly anharmonic motion of the molecule, some kind of conformational fluctuations", and the insert in their Figure 1 shows their analysis in the form of the temperature dependence of the rescaled intensity. The second is at ≈230 K, close to the so-called crossover temperature (T_c) of water,[87] and this is a temperature range where many hydrated biopolymers show strong slowing down of their functions. Sokolov et al.[55] speculate that "the hydration shell has critical behavior in the dynamics at $T \approx 210-230$ K and the motion of biomolecules is coupled to the surrounding water. As a result the hydration shell hinders the motion of macromolecules and suppresses their function".

Our study can be connected with their results and supports their speculations on the role of the hydration shell for the low-temperature dynamics of biomolecules. A basic difference between the approach of Sokolov et al. and ours is, first, the difference in the time scales of the experiments. Second, and more important, our approach is to generate a nonequilibrated sample by rapid cooling into the glassy state and then to follow isothermal relaxation toward equilibrium, whereas the hydrated LiDNA sample studied by Sokolov et al.[55] probably had equilibrated on heating to 200 K. We draw this conclusion because at 200 K τ_a of similarly hydrated B-DNA samples is ≈10 min,[9] and it depends only to a minor degree on the length of the DNA.[9] Because the LiDNA sample apparently had been cooled slowly and measurement time is long in inelastic neutron scattering experiments, τ_a of ≈10 min at 200 K gives ample time for equilibration.

If this is true, which process is causing the onset of dynamics observable in their Figure 1 at ≈180−200 K? We suggest that the "conformational fluctuations" ascribed to by Sokolov et al.[55] are in fact the B_I/B_{II} interconversion in an *equilibrated* sample coupled with restructuring of their hydration shells which becomes sufficiently dynamic to cause, at a given temperature, the effect observable in their Figure 9. Furthermore, on heating B-DNA from 200 to 290 K, the equilibrated B_{II}/B_I population ratio increases by a factor of ≈2 (cf. our Figure 2). This factor could be different for other forms of B-DNA, but an increasing B_{II} population with increasing temperature seems to be general, as observed for native polymeric B-DNA.[7−9,12] It is possible that this increasing amount of B_{II} with temperature causes additional anharmonicity and thus contributes to the increasing intensity shown in their Figure 9 insert.

The two distinct temperature regions at ≈180−200 K and at ≈230 K observed by Sokolov et al.[55] in apparently equilibrated samples are also the temperature regions where we observe, or assume, dynamic effects in nonequilibrated, fast-cooled samples. The first is the temperature region where we can follow isothermal relaxation toward equilibrium via $B_I \rightarrow B_{II}$ interconversion (cf. Figure 2),[7−13] and the second is the temperature region of ≈220−240 K where on fast-cooling we assume slowing down and freezing-in of the hydration shells of the B_I

and B_{II} substates. These temperature ranges obviously depend to some extent on the rate of cooling. Nevertheless, they are consistent with speculations pointed out above that the low-temperature limit of biological function is caused by slowing down and freezing-in of the dynamics of the hydration shell. These speculations on the origin of the low-temperature functions of DNA and of proteins in terms of slowing-down of hydration shell dynamics are discussed and reviewed by Sokolov et al.[55] within the concepts of modern glass transition theory and the energy landscape paradigm.[88−90] It seems surprising that the onset of anharmonicity in an equilibrated sample and relaxation effects in terms of $B_I \rightarrow B_{II}$ interconversion in nonequilibrated B-DNA should occur at similar temperatures. Angell[91] has addressed this apparent problem for the low-temperature dynamics in proteins and shown that it "is largely resolved by recognizing how narrow is the range of temperature over which the relaxation time changes from small to very large values," and thus, the temperature difference is only minor (see inset to Figure 11 in ref 91). The onset of anharmonicity can be viewed as a precursor for the real glass transition characterized by the heat capacity jump.

It seems possible that the "200 K glasslike transition" observed in proteins has the same origin, in that on cooling from the liquid state to the glassy state first slowing down of hydration shell dynamics occurs and exchange between conformational substates is frozen-in at much lower temperatures. A basic difference is that "proteins can assume a large number of nearly isoenergetic conformations (conformational substates)",[92] whereas in B-DNA, we observed only two, namely, B_I and B_{II}. Therefore, unravelling of the various processes in a manner similar to Figure 2 will be much more difficult. Here again it seems to be important to distinguish between dynamics in slow-cooled (nearly) equilibrated samples[66−81] and that in fast-cooled nonequilibrated samples.[82−86] First results of the effects of cooling rate and thermal history on the low-temperature dynamics of haemoglobin were obtained recently by quasielastic neutron spectroscopy.[81]

Conclusions

Whereas the equilibrium substate population of hydrated B-DNA with $\Gamma = 13$ (or 14) is identical for slow-cooled and fast-cooled hydrated DNA after relaxation at 200 K, the nonequilibrium populations are not. Normally one would expect the nonequilibrium population of a fast-cooled sample to be more similar to the equilibrated state at 300 K because substates become frozen-in (cf. Figure 2). Here we observe the contrary; that is, the fast-cooled sample deviates more from the 300 K population. This means that fast-cooled B-DNA is relaxing toward a different state and at a higher rate during the cooling process than slow-cooled DNA. A possible explanation for this surprising result can be found by considering the hydration shell whose kinetics is apparently different from the kinetics of B-DNA's substate interconversion. Once hydrated DNA with $\Gamma = 13$ (14) is cooled, its hydration shell does deviate from the equilibrium line at different temperatures, depending on the cooling rate, leading to a path-dependent hydration environment. DNA trapped inside its hydration water has specific kinetic and thermodynamic properties governed by its hydration shell. We believe that this is a reasonable explanation for our results presented here.

What are the implications? Other conformational transitions may be influenced by hydration water as well, e.g., base-pair opening and sugar repuckering. Residence times of water molecules in hydration shells of proteins and nucleic acids were found to be in the range of microseconds to nanoseconds.[93,94] Conformational exchange happens on different time scales, ranging from nanoseconds to milliseconds. It seems likely that conformational transitions faster than the residence time of water are governed by the dynamics of the hydration layer. This has numerous implications, not only for nucleic acids but also for proteins' molecular function and recognition. Pronounced slowing-down of the hydration shell dynamics occurs at ≈220 to ≈240 K; therefore, slowed kinetics of hydration water becomes dominant at these temperatures and below.[55] For water trapped inside a biomolecule or at the biomolecule−ligand interface, the glasslike transition temperature can be considerably higher.[93,95,96] This implies the importance of water on all sorts of biological mechanisms. Inconsistencies between experimental data acquired at different temperatures and not completely attributable to the dynamics of the biomolecule itself may find an explanation based on our observations.

Acknowledgment. We are grateful for financial support by the "Foschungsförderungsfonds" of Austria (Project No. 12319-PHY).

References and Notes

(1) Texter, J. *Prog. Biophys. Mol. Biol.* **1978**, *33*, 83−97.
(2) Saenger, W. *Principles of Nucleic Acid Structure*; Springer-Verlag: New York, 1984.
(3) Westhof, E. *Annu. Rev. Biophys. Biophys. Chem.* **1988**, *17*, 125−144.
(4) Jeffrey, G. A.; Saenger, W. *Hydrogen Bonding in Biological Structures*; Springer-Verlag: New York, 1994.
(5) Berman, H. M. *Curr. Opin. Struct. Biol.* **1994**, *4*, 345−350.
(6) Berman, H. M.; Schneider, B. Nucleic acid hydration. In *Nucleic Acid Structure*; Neidle, S., Ed.; Oxford University Press: Oxford, U.K., 1999; pp 295−312.
(7) Rüdisser, S.; Hallbrucker, A.; Mayer, E. *J. Am. Chem. Soc.* **1997**, *119*, 12251−12256.
(8) Pichler, A.; Rüdisser, S.; Mitterböck, M.; Huber, C. G.; Winger, R. H.; Liedl, K. R.; Hallbrucker, A.; Mayer, E. *Biophys. J.* **1999**, *77*, 398−409.
(9) Rüdisser, S.; Pichler, A.; Winger, R. H.; Liedl, K. R.; Hallbrucker, A.; Mayer, E. *J. Mol. Liquids* **2000**, *86*, 137−149.
(10) Pichler, A. FT-IR-spektroskopische Untersuchung der Konformationsunterzustände B_I und B_{II} von B-DNA im d(CGCGAATTCGCG)$_2$ Dodekamer und in DNA aus Lachshoden, University of Innsbruck, 1999.
(11) Pichler, A.; Hallbrucker, A.; Winger, R. H.; Liedl, K. R.; Mayer, E. *J. Phys. Chem. B* **2000**, *104*, 11354−11359.
(12) Pichler, A.; Rüdisser, S.; Winger, R. H.; Liedl, K. R.; Hallbrucker, A.; Mayer, E. *Chem. Phys.* **2000**, *258*, 391−404.
(13) Pichler, A.; Rüdisser, S.; Winger, R. H.; Wellenzohn, B.; Flader, W.; Liedl, K. R.; Hallbrucker, A.; Mayer, E. *Appl. Spectrosc.* **2001**, *55*, 9−22.
(14) Winger, R. H.; Liedl, K. R.; Rüdisser, S.; Pichler, A.; Hallbrucker, A.; Mayer, E. *J. Phys. Chem. B* **1998**, *102*, 8934−8940.
(15) Winger, R. H.; Liedl, K. R.; Pichler, A.; Hallbrucker, A.; Mayer, E. *J. Biomol. Struct. Dynamics* **1999**, *17*, 223−235.
(16) Winger, R. H.; Liedl, K. R.; Pichler, A.; Hallbrucker, A.; Mayer, E. *J. Phys. Chem. B* **2000**, *104*, 11349−11353.
(17) Hong, M. K.; Braunstein, D.; Cowen, B.; Frauenfelder, H.; Iben, I. E. T.; Mourant, J. R.; Ormos, P.; Scholl, R.; Schulte, A.; Steinbach, P. J.; Xie, A.-H.; Young, R. D. *Biophys. J.* **1990**, *58*, 429−436.
(18) Potter, W. T.; Hazzard, J. H.; Choc, M. G.; Tucker, M. P.; Caughey, W. S. *Biochemistry* **1990**, *29*, 6283−6295.
(19) Hogan, M. E.; Jardetzky, O. *Proc. Natl. Acad. Sci.* **1979**, *76*, 6341−6345.
(20) Chou, S.-H.; Cheng, J.-W.; Reid, B. R. *J. Mol. Biol.* **1992**, *228*, 138−155.
(21) Gorenstein, D. G. *Chem. Rev.* **1994**, *94*, 1315−1338.
(22) Tisne, C.; Hantz, E.; Hartmann, B.; Delepierre, M. *J. Mol. Biol.* **1998**, *279*, 127−142.
(23) Rüdisser, S.; Hallbrucker, A.; Mayer, E. *J. Phys. Chem.* **1996**, *100*, 458−461.
(24) Rüdisser, S.; Hallbrucker, A.; Mayer, E.; Johari, G. P. *J. Phys. Chem.* **1997**, *101*, 266−277.
(25) Rüdisser, S.; Fleissner, G.; Pichler, A.; Hallbrucker, A.; Mayer, E. *J. Mol. Struct.* **1999**, *479*, 237−243.
(26) Dickerson, R. E.; Drew, H. R. *J. Mol. Biol.* **1981**, *149*, 761−786.

(27) Drew, H. R.; Dickerson, R. E. *J. Mol. Biol.* **1981**, *151*, 535−556.
(28) Drew, H. R.; Wing, R. M.; Takano, T.; Broka, C.; Tanaka, S.; Itakura, K.; Dickerson, R. E. *Proc. Natl. Acad. Sci.* **1982**, *78*, 2179−2183.
(29) Wing, R.; Drew, H.; Takano, T.; Broka, C.; Tanaka, S.; Itakura, K.; Dickerson, R. E. *Nature* **1980**, *287*, 755−758.
(30) Dickerson, R. E. Helix structure and molecular recognition by B-DNA. In *Nucleic Acid Structure*; Neidle, S., Ed.; Oxford University Press: Oxford, U.K., 1998; pp 145−197.
(31) Pichler, A.; Rüdisser, S.; Winger, R. H.; Liedl, K. R.; Hallbrucker, A.; Mayer, E. *J. Am. Chem. Soc.* **2000**, *122*, 716−717.
(32) Whitka, J. M.; Swaminathan, S.; Srinivasan, J.; Beveridge, D. L.; Bolton, P. H. *Science* **1992**, *255*, 597−599.
(33) Denisov, V. P.; Carlström, G.; Venu, K.; Halle, B. *J. Mol. Biol.* **1997**, *268*, 118−136.
(34) Lane, A. N.; Jenkins, T. C.; Brown, T.; Neidle, S. *Biochemistry* **1991**, *30*, 1372−1385.
(35) Robinson, B. H.; Mailer, C.; Drobny, G. *Annu. Rev. Biophys. Biomol. Struct.* **1997**, *26*, 629−658.
(36) Hatcher, M. E.; Mattiello, D. L.; Meints, G. A.; Orban, J.; Drobny, G. P. *J. Am. Chem. Soc.* **1998**, *120*, 9850−9862.
(37) Weidlich, T.; Lindsay, S. M.; Rui, Q.; Rupprecht, A.; Peticolas, W. L.; Thomas, G. A. *J. Biomol. Struct. Dyn.* **1990**, *8*, 139−171.
(38) Kubasek, W. L.; Wang, Y.; Thomas, G. A.; Patapoff, T. W.; Schoenwaelder, K.-H.; Van der Sande, J. H.; Peticolas, W. L. *Biochemistry* **1986**, *25*, 7440−7445.
(39) Peticolas, W. L.; Thomas, G. A.; Wang, Y. *J. Mol. Liquids* **1989**, *41*, 367−388.
(40) Taillandier, E. *Nucleic Acid Conformations Studied by Vibrational Spectroscopy*; Adenine Press: Schenectady, NY, 1990; Vol. 3.
(41) Taillandier, E.; Liquier, J. *Methods Enzymol.* **1992**, *211*, 307−335.
(42) Poncin, M.; Hartmann, B.; Lavery, R. *J. Mol. Biol.* **1992**, *226*, 775−794.
(43) Hartmann, B.; Piazolla, D.; Lavery, R. *Nucleic Acids Res.* **1993**, *21*, 561−568.
(44) Bertrand, H.-O.; Ha-Duong, T.; Fermandjian, S.; Hartmann, B. *Nucleic Acids Res.* **1998**, *26*, 1261−1267.
(45) Young, M. A.; Ravishanker, G.; Beveridge, D. L. *Biophys. J.* **1997**, *73*, 2313−2336.
(46) Young, M. A.; Jayaram, B.; Beveridge, D. L. *J. Am. Chem. Soc.* **1997**, *119*, 59−69.
(47) Duan, Y.; Wilkosz, P.; Crowley, M.; Rosenberg, J. M. *J. Mol. Biol.* **1997**, *272*, 553−572.
(48) Fratini, A. V.; Kopka, M. L.; Drew, H. R.; Dickerson, R. E. *J. Biol. Chem.* **1982**, *257*, 14686−14707.
(49) Cruse, W. B. T.; Salisbury, S. A.; Brown, T.; Cosstick, R.; Eckstein, F.; Kennard, O. *J. Mol. Biol.* **1986**, *192*, 891−905.
(50) Privé, G. G.; Heinemann, U.; Chandrasegaran, S.; Kan, L.-S.; Kopka, M. L.; Dickerson, R. E. *Science* **1987**, *238*, 498−504.
(51) Grzeskowiak, K.; Yanagi, K.; Prive, G. G.; Dickerson, R. E. *J. Biol. Chem.* **1991**, *266*, 8861−8883.
(52) Dickerson, R. E.; Goodsell, D. S.; Kopka, M. L.; Pjura, R. E. *J. Biomol. Struct. Dyn.* **1987**, *5*, 557−579.
(53) Clark, G. R.; Squire, C. J.; Baker, L. J.; Martin, R. F.; White, J. *Nucleic Acids Res.* **2000**, *28*, 1259−1265.
(54) van Dam, L.; Levitt, M. H. *J. Mol. Biol.* **2000**, *304*, 541−561.
(55) Sokolov, A. P.; Grimm, H.; Kahn, R. *J. Chem. Phys.* **1999**, *110*, 7053−7057.
(56) Taillandier, E.; Liquier, J.; Taboury, J. A. Infrared Spectral Studies Of DNA Conformations. In *Advances in Infrared and Raman Spectroscopy*; Clark, R. J. H., Hester, R. E., Eds.; Wiley: New York, 1985; Vol. 12, pp 65−114.
(57) Huber, C. G.; Oefner, P. J.; Bonn, G. K. *Anal. Chem.* **1995**, *67*, 578−585.
(58) Falk, M.; Hartman Jr., K. A.; Lord, R. C. *J. Am. Chem. Soc.* **1962**, *85*, 391−394.
(59) Falk, M.; Poole, A. G.; Goymour, C. G. *Can. J. Chem.* **1970**, *48*, 1536−1539.
(60) Bertie, J. E.; Labbe, H. J.; Whalley, E. *J. Chem. Phys.* **1969**, *10*, 4501−4520.
(61) Walrafen, G. E.; Yang, W.-H.; Chu, Y. C. *J. Phys. Chem. B* **1999**, *103*, 1332−1338.
(62) Kuntz, J. I. D.; Brassfield, D. S.; Law, G. D.; Purcell, G. V. *Science* **1969**, *163*, 1329−1331.
(63) Bloomfield, V. A.; Crothers, D. M.; Tinoco, J. I. *Nucleic Acids. Structures, Properties, and Functions*; University Science Books: Sausalito, CA, 2000.
(64) Wolf, B.; Hanlon, S. *Biochemistry* **1975**, *14*, 1661−1670.
(65) Liquier, J.; Taillandier, E. Infrared Spectroscopy Of Nucleic Acids. In *Infrared Spectroscopy of Biomolecules*; Mantsch, H. H., Chapman, D., Eds.; Wiley-Liss: New York, 1996; pp 131−158.
(66) Morozov, V. N.; Gevorkian, S. G. *Biopolymers* **1985**, *24*, 1785−1799.
(67) Frauenfelder, H.; Gratton, E. *Methods Enzymol.* **1986**, *127*, 207−216.
(68) Parak, F. *Methods Enzymol.* **1986**, *127*, 196−206.
(69) Doster, W.; Bachleitner, A.; Dunau, R.; Hiebl, M.; Lüscher, E. *Biophys. J.* **1986**, *50*, 213−219.
(70) Doster, W.; Cusack, S.; Petry, W. *Nature* **1989**, *337*, 754−756.
(71) Doster, W.; Cusack, S.; Petry, W. *Phys. Rev. Lett.* **1990**, *65*, 1080−1084.
(72) Nienhaus, G. U.; Heinzl, J.; Huenges, E.; Parak, F. *Nature* **1989**, *338*, 665−666.
(73) Goldanskii, V. I.; Krupyanskii, Y. F. *Q. Rev. Biophys.* **1989**, *22*, 39−92.
(74) Smith, J.; Kuczera, K.; Karplus, M. *Proc. Natl. Acad. Sci. U.S.A.* **1990**, *87*, 1601−1605.
(75) Rupley, J. A.; Careri, G. *Adv. Protein Chem.* **1991**, *41*, 37−172.
(76) Srajer, V.; Reinisch, L.; Champion, P. M. *Biochemistry* **1991**, *30*, 4886−4893.
(77) Champion, P. M. *J. Raman Spectrosc.* **1992**, *23*, 557−567.
(78) Pethig, R. *Annu. Rev. Phys. Chem.* **1992**, *43*, 177−205.
(79) Pissis, P.; Anagnostopoulou-Konsta, A.; Apekis, L.; Daoukaki-Diamanti, D.; Christodoulides, C. *IEEE Trans. Elect. Insulation* **1992**, *27*, 820−825.
(80) Mayer, E. *Biophys. J.* **1994**, *67*, 862−873.
(81) Tengroth, C.; Börjesson, L.; Kagunya, W. W.; Middendorf, H. D. *Physica B* **1999**, *266*, 27−34.
(82) Sartor, G.; Hallbrucker, A.; Hofer, K.; Mayer, E. *J. Phys. Chem.* **1992**, *96*, 5133−5138.
(83) Sartor, G.; Mayer, E.; Johari, G. P. *Biophys. J.* **1994**, *66*, 249−258.
(84) Green, J. L.; Fan, J.; Angell, C. A. *J. Phys. Chem.* **1994**, *98*, 13780−13790.
(85) Sartor, G.; Johari, G. P. *J. Phys. Chem.* **1996**, *100*, 10450−10463.
(86) Johari, G. P.; Sartor, G. *J. Chem. Soc., Faraday Trans.* **1996**, *92*, 4521−4531.
(87) Sokolov, A. P.; Hurst, J.; Quitmann, D. *Phys. Rev. B* **1995**, *51*, 12865−12868.
(88) Goldstein, M. *J. Chem. Phys.* **1969**, *51*, 3728−3739.
(89) Stillinger, F. H. *Science* **1995**, *267*, 1935−1939.
(90) Debenedetti, P. G.; Stillinger, F. H. *Nature* **2001**, *410*, 259−267.
(91) Angell, C. A. *Science* **1995**, *267*, 1924−1935.
(92) Frauenfelder, H.; Sligar, S. G.; Wolynes, P. G. *Science* **1991**, *254*, 1598−1603.
(93) Denisov, V. P.; Halle, B. *Faraday Discuss.* **1996**, *103*, 227−244.
(94) Denisov, V. P.; Carlström, G.; Venu, K.; Halle, B. *J. Mol. Biol.* **1997**, *268*, 118−136.
(95) Wang, Y.-X.; Freedberg, D. I.; Grzesiek, S.; Torchia, D. A.; Wingfield, P. T.; Kaufman, J. D.; Stahl, S. J.; Chang, C.-H.; Hodge, C. N. *Biochemistry* **1996**, *35*, 12694−12704.
(96) Bizzarri, A. R.; Paciaroni, A.; Cannistraro, S. *Phys. Rev. E* **2000**, *62*, 3991−3999.